An Investigation of RANS Simulations for Swirl-Stabilized Isothermal Turbulent Flow in a Gas Turbine Burner

Open Access

Tariq Md Ridwanur Rahman[1], Waqar Asrar[1,*], Sher Afghan Khan[1]

1   Department of Mechanical Engineering, International Islamic University Malaysia, 53100 Kuala Lumpur, Malaysia.

ARTICLE INFO	ABSTRACT
	The presence of complex flow features in swirling flows have made it an essential part of many engineering applications. These features can only be accurately predicted by the DNS or LES type methods which are highly expensive in terms of resources and time. This fact established the RANS approach as the key method in the industrial arena because of its modest requirement of resources unlike LES. However, existing RANS investigations on swirl-stabilized isothermal turbulent flow are 2D and lack credibility on the question of predicting the prominent flow features which exist in swirling flows. The current study investigates the 3D RANS simulations in predicting a swirl-stabilized isothermal turbulent flow in a burner for a gas-turbine combustion chamber which possesses complex flow features such as bluff-body induced recirculation zone and Vortex Breakdown (VB) bubble. Current investigations also assess the establishment of 3D RANS simulations as a viable industrial alternative to the computationally expensive LES and the less accurate 2D RANS simulations. Furthermore, the influence of mesh quality, different turbulence models, discretization schemes on the accuracy of the predictions are examined. It was found that the multi-zonal mesh with hexahedron cells had the highest mesh quality and produced the best results, and the standard k-ϵ model predicted all the flow features with default schemes in ANSYS-Fluent. The conclusions in the paper are valuable, practical and will save a lot of time and effort of practicing engineers during the numerical modelling setup selection stages for solving such complex three-dimensional flow problems.

1. Introduction

Swirling flows, both the reacting and the non-reacting, are complex in nature but have features that make them attractive to use in many practical applications [1-3], such as internal combustion engines, gas turbines [1], burners, chemical processing plants, rotary kilns, spray dryers [2], power station combustors, furnaces and boilers [4]. Depending on the degree (or strength) of the swirl and the furnace and burner geometry, it is possible to achieve different recirculation patterns and vortex breakdown regimes [3, 4, 5] which provide a source of substantially mixed combustion products and

*   *Corresponding author.*
E-mail address: waqar@iium.edu.my (Waqar Asrar)

acts as a storage of heat and chemically active species to sustain combustion and provide flame stabilization [1, 4, 6] and minimization of pollutants [1, 3, 6].

Swirl-stabilized flows and flames have been studied in many experimental investigations such as the TNF (Turbulent Non-premixed Flames) workshop [7] which has a well-established experimental database of turbulent non-premixed flame configurations comprising of: 1) simple jet, 2) bluff-body stabilized flames, and 3) swirl-stabilized flames. Among these, the swirl-stabilized flame configuration has been found to be the most challenging test case to assess the validity of different turbulence and combustion models [8] due to the presence of two recirculation zones in a specific combination of low swirl number and higher primary axial velocity as compared to the bluff-body stabilized flows, which has only one recirculation zone [2, 9].

The TNF workshop project includes the Sydney swirl project [10] which has reliable experimental test cases covering a range of swirl numbers for two isothermal or non-reacting swirling flow cases and eight reacting swirling flow cases of three different types of fuels. Experimental results of both cases have been reported in detail in different publications [1-3, 9, 11-15] and has been taken as the test case for the current numerical investigations.

Numerical investigations have been undertaken by several research groups on isothermal swirling flow cases as well as swirling flame cases. Most of these numerical investigations were carried out using in-house codes, however a few cases of commercial CFD package usage [16, 17] has also been reported in published literature.

Most recent work on the swirl flow and flame cases has been conducted by Safavi and Amani [8] who carried out a comparative study of different steady and unsteady turbulence models including different 2D RANS models (RNG k-ϵ, SST k-ω, Transition-SST, and Reynolds stress model) along with LES (Germano's dynamic SGS) as well as 3D Hybrid models (SST k-ω based Scale-adaptive simulation (SAS), Realizable k-ϵ based Detached eddy simulation (DES), and SST k-ω based DES). The results focused on the prediction of the flow features like the vortex breakdown (VB) bubble and the flow field in general.

Similar comparative studies in 2D axisymmetric domains were carried out by Radwan *et al.,* [16] using standard and realizable k-ϵ, standard k-ω, and Reynolds stress model (RSM) while De Meester *et al.,* used non-linear k-ϵ model as well [18]. The investigations focused primarily on the comparison of general flow pattern predictions with experimental data. Gupta and Kumar [19] studied swirling flow inside a cylinder using particle tracking velocimetry (PTV) and 3D k-ϵ models. The study compared the results from the RNG k-ϵ and the standard k-ϵ model. West *et al.,* [20] compared SST based DES model performance with LES and 2D unsteady RANS models in the prediction of mean and fluctuating velocity components. Widenhorn *et al.,* [21] benchmarked turbulence models of the commercial CFD software package ANSYS CFX and compared the SST based SAS model with the SST based DES model.

Reynolds stress model (RSM), standard k-ϵ, and an algebraic stress model (ASM) were tested in a near-burner zone by Weber *et al.,* [22] for axisymmetric 2D computational domain. They observed that in the burner quarl where inviscid expansion of flow takes place, the k-ϵ model introduces considerable amount of error. Wegner *et al.,* [23] investigated 3D flow configuration in a non-premixed swirl burner that is widely studied in the well-known TECFLAM project [24]. They compared the result of URANS simulation with experimental data and LES results.

Apart from the two-equation based simulations, several LES studies have also been carried out such as the one by Wu *et al.,* [25] where the effect of outlet geometry contraction on the vortex breakdown (VB) structure was examined. Dinesh *et al.,* [26] carried out an LES investigation to model a turbulent confined cannular combustor and examined the effects of swirling flow on mixing and the flow field. LES study by Bulat *et al.,* [27] examined an isothermal strong swirling confined flow in

the combustion chamber of the industrial gas turbine Siemens SGT-100 at different Reynolds number. The obtained results are compared with the experimental data from the TURCHEMI project [28]. Good agreement with the experimental data of the Sydney swirl burner has been shown in many LES works for both turbulent non-reacting [4, 5, 17, 29-34] and reacting flow cases [6, 29-31, 33, 35-39]. These covered detailed investigations on different important characteristics of swirling flow, i.e. swirl-stabilized recirculation zones- particularly vortex breakdown (VB) bubble, intermittency, jet precession. From these LES works, the findings on swirl-stabilized recirculation zones are reported in detail in Table 9 and compared with the results of the current investigations. However, LES is not preferred in industry-based works as this technique is time consuming and computationally expensive. Rather, in the last few decades the RANS approach has been the key technique in industrial CFD applications as it is computationally inexpensive and requires less computation time than the LES approach [40].

The literature survey conducted in this work has revealed that 2D axisymmetric RANS simulations are inadequate in capturing the main flow features of the swirl-stabilized isothermal turbulent flow inside a burner. The recirculation zones such as the vortex breakdown (VB) bubble are 3D in nature and 2D approach is unlikely to capture the flow physics of these zones. Therefore, a 3D approach is more suitable and needs to be investigated comprehensively in the RANS framework. The few 3D RANS studies reported in published literature focused mainly on predicting the velocity trends in the different zones of the flow regime. The current work will therefore concentrate mainly on the capability of 3D RANS schemes in capturing the prominent flow features of the swirl-stabilized isothermal turbulent flow. Additionally, the influence of numerical issues like mesh refinement in critical zones, mesh structure, discretization schemes, and different turbulence models on the accurate prediction of prominent flow features will be evaluated with the objective of assessing 3D RANS simulations as a viable and inexpensive alternative to the time consuming and computationally expensive LES approach.

2. Problem Description

The isothermal swirl-stabilized turbulent flow considered in this study corresponds to the Sydney swirl burner [2, 9, 10] and the physical domain is shown in Figure 1.
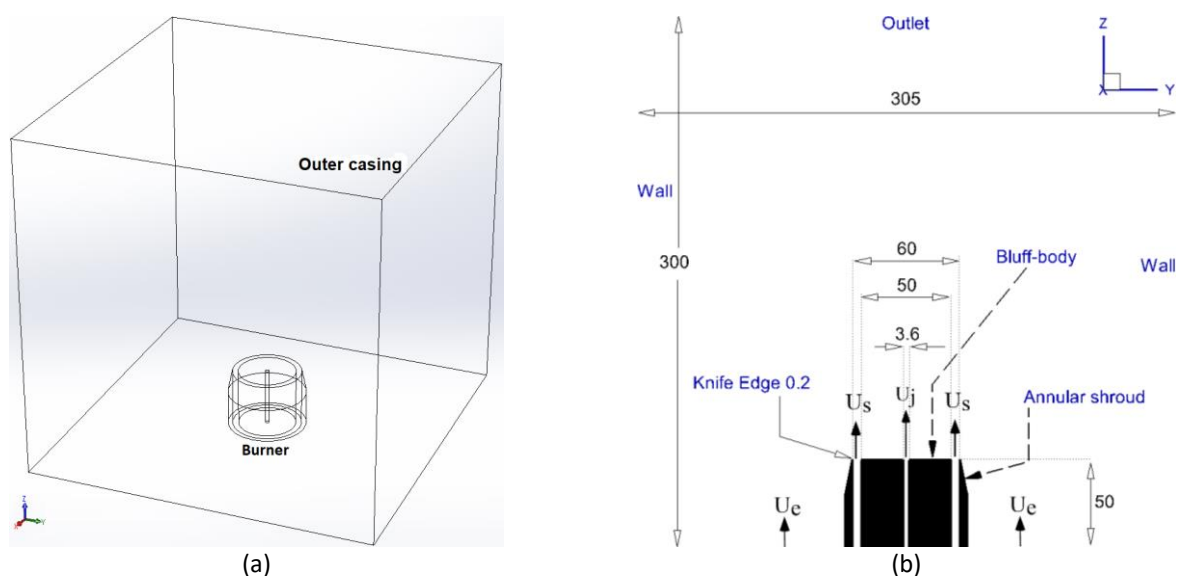
Fig. 1. Physical domain of the isothermal swirl-stabilized turbulent flow. All measurements are in mm

The burner consists of a 50 mm diameter cylindrical bluff-body with a 3.6 mm diameter hole injecting the fuel jet (U_j). A 10 mm thick annulus surrounding the bluff-body introduces a swirling flow (U_s: Axial component, W_s: Tangential component) into the physical domain. The strength of the swirl is characterized by the geometric swirl number, $S_g = W_s/U_s$, defined according to Kalt *et al.,* [1]. The swirl number can be varied by changing the magnitudes of the tangential and axial components [12]. A 60 mm diameter annulus shroud surrounds the bluff-body with a knife edge of 0.2 mm thickness at the exit plane. The burner is housed inside a square outer casing with a cross section of 305 mm × 305 mm where a secondary axial co-flow (U_e) exists.

The specific velocity and swirl number values that will be used in this study are listed in Table 1.

Table 1
Physical parameters of the low-swirl isothermal
flow N29S054 case [2, 10]

U_j (m/s)	U_s (m/s)	W_s (m/s)	S_g	U_e (m/s)
66	29.74	16.0596	0.54	20

The prominent flow features include a recirculation zone induced by the bluff-body, and the eventual occurrence of a downstream recirculation zone at the center due to vortex breakdown (VB) bubble phenomena. The successful simulation of such a sensitive configuration can be considered as an important milestone for the RANS simulation technique, which will be attempted in this study.

3. Computational Details

The governing equations comprise of continuity and momentum as listed below

$$\frac{\partial}{\partial x_i}(\rho u_i) = 0 \tag{1}$$

$$\frac{\partial}{\partial x_j}(\rho u_i u_j) = -\frac{\partial p}{\partial x_i} + \frac{\partial}{\partial x_j}\left[\mu\left(\frac{\partial u_i}{\partial x_j} + \frac{\partial u_j}{\partial x_i} - \frac{2}{3}\delta_{ij}\frac{\partial u_l}{\partial x_l}\right)\right] + \frac{\partial}{\partial x_j}\left(-\rho\overline{u_i' u_j'}\right) \tag{2}$$

The closure for the Reynolds stresses $-\rho\overline{u_i' u_j'}$ is specified by the Boussinesq approximation.

$$-\rho\overline{u_i' u_j'} = -\frac{2}{3}k\delta_{ij} + \mu_t\left(2S_{ij}\right) \tag{3}$$

where,

$$S_{ij} = \frac{1}{2}\left(\frac{\partial u_i}{\partial x_j} + \frac{\partial u_j}{\partial x_i}\right) \tag{4}$$

The turbulent viscosity μ_t is specified in the standard k-ϵ model as follows

$$\mu_t = c_\mu f_\mu \frac{k^2}{\epsilon} \tag{5}$$

The kinetic energy k and the turbulent dissipation rate ϵ are determined by solving their respective transport equations [41].

The governing equations were discretized on two types of mesh: tetrahedron and hexahedron setup in the physical domain. Single and multi-zone meshes are implemented in order to assess the influence of mesh refinement in capturing the bluff-body induced recirculation zone and the vortex breakdown (VB) recirculation bubble which are reported as the main flow features of the swirl-stabilized isothermal turbulent flow in the experimental and unsteady numerical investigations. A total of five different configurations of mesh type and zones are investigated in this study as listed in Table 2.

Table 2
Meshes investigated in current study

Mesh code	Cell shape of Mesh	Number of zones	Number of cells (in million)
T1	Tetrahedron	1	1.67
T5	Tetrahedron	5	1.73
H5	Hexahedron	5	2.29
T10	Tetrahedron	10	3.42
H10	Hexahedron	10	3.45

Structures of the single and multi-zone mesh in the computational domain is shown in Figure 2 where zoning of the meshes are indicated by red lines.

The solution of the governing Eqs. (1-5) on the different meshes shown in Figure 2 are obtained using the ANSYS-Fluent solver which uses the Finite Volume Method (FVM) for numerical discretization along with the SIMPLE algorithm for the pressure coupling. In order to predict the flow field using the standard k-ϵ model, different spatial discretization schemes are tested to ascertain their accuracy and are listed in Table 3.

All simulations are run for 7700 iterations using the double-precision solver of ANSYS-Fluent. A combination of FFF and SSS schemes (FFF+SSS) was also investigated in which the FFF scheme was run for 2200 iterations and the obtained solution was used to initialize the SSS scheme which was run for an additional 5500 iterations resulting in a total of 7700 iterations. The solutions are considered converged when all residuals drop below 10^{-6}.

Additionally, five other variants of turbulence models are tested in this study. The different turbulence models employed in this investigation are listed in Table 4.

Table 3
Upwind schemes for spatial discretization for the standard k-ϵ model used in current study

Scheme code	Momentum	Turbulent kinetic energy (k)	Turbulent dissipation rate (ϵ)
SFF (default)	Second order	First order	First order
SSS	Second order	Second order	Second order
FFF	First order	First order	First order

Table 4
Different turbulence models used in this study

Model	Description
k-ϵ	2-equation standard k-ϵ
k-ϵ	2-equation RNG k-ϵ
k-ϵ	2-equation realizable k-ϵ
k-ω	2-equation standard k-ω
T-SST	4-equation Transition-SST
RSM	7-equation stress-ω Reynolds stress model

(a) T1 mesh

(b) T5 mesh

(c) H5 mesh

(d) T10 mesh

(e) H10 mesh
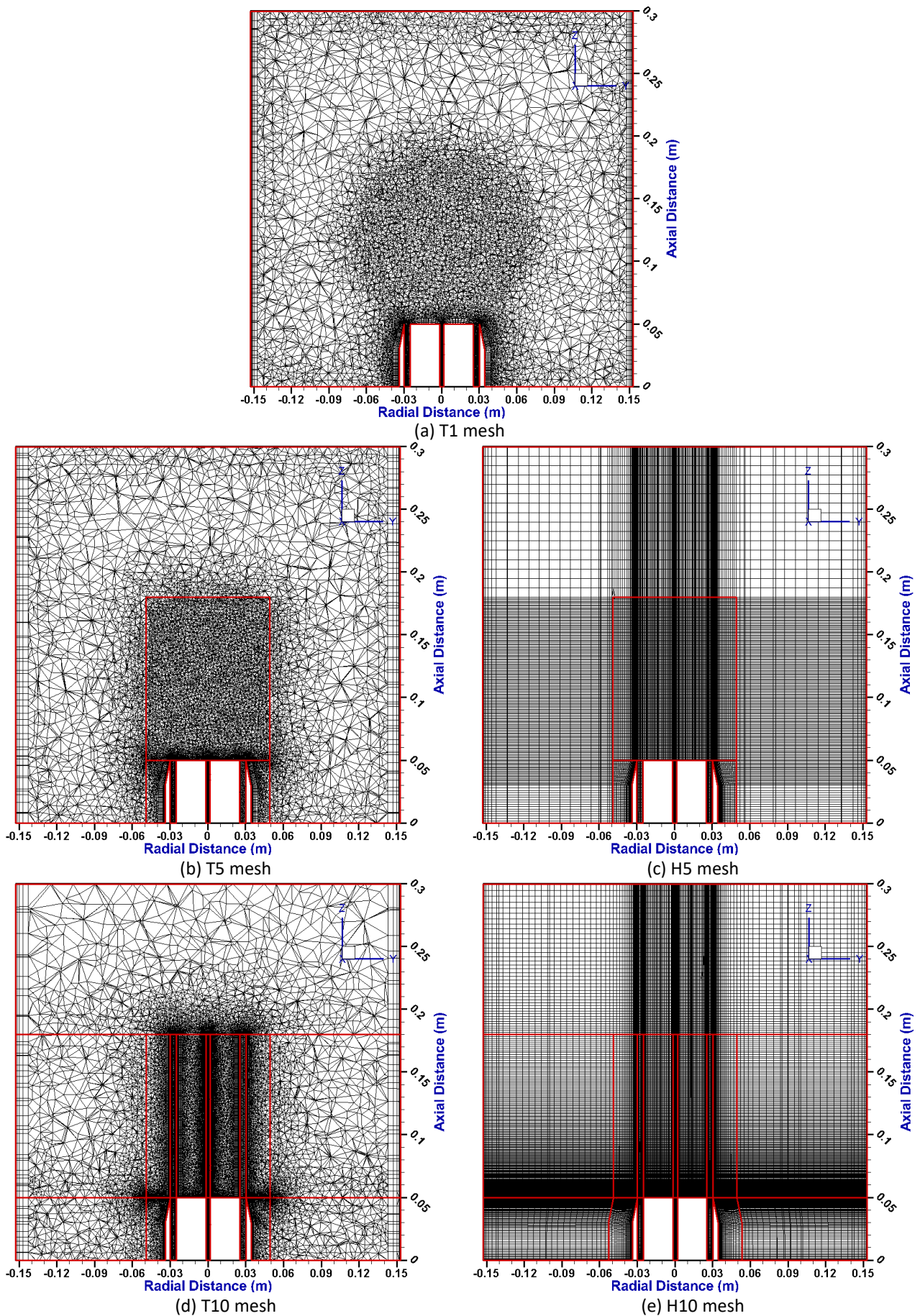
Fig. 2. Structures of different meshes at the centerline YZ-plane with zones indicated in red

4. Results and Discussions

One of the main objectives of this investigation is to study the influence of mesh quality and structure on the prediction of the prominent flow features such as the bluff-body induced recirculation zone and vortex breakdown (VB) bubble. Towards fulfilling this objective, two mesh metrics- Orthogonal Quality and Skewness are calculated to gauge the quality of the different mesh structures used in this study and the results are presented in Table 5.

Table 5
Mesh Quality of different meshes used in this study. 'SD' denotes Standard Deviation

Mesh Metric	Statistics	T1 mesh	T5 mesh	H5 mesh	T10 mesh	H10 mesh
	Min	6.70E-02	1.83E-02	6.72E-01	6.65E-02	7.07E-01
Orthogonal	Max	0.9999911	0.9999808	0.9999999	0.9999813	0.9999999
Quality	Average	0.899	0.876	0.985	0.901	0.984
	SD	0.097	0.125	0.038	0.101	0.044
	Min	5.098E-05	1.082E-05	4.507E-05	1.381E-05	4.262E-06
	Max	0.94	0.982	0.769	0.933	0.597
Skewness	Average	0.183	0.217	0.078	0.191	0.076
	SD	0.139	0.157	0.106	0.137	0.103

It can be observed from Table 4 that the hexahedron meshes; H5 and H10 are the best in terms of average orthogonal quality (0.985 and 0.984 respectively). Additionally, the SD values for H5 and H10 meshes are also similar (0.03881 and 0.044). However, the H10 mesh has a lower average skewness value (0.076) as compared to the corresponding H5 mesh value (0.078). Therefore, the H10 mesh can be regarded as the better quality mesh and likely to produce better results. The prediction of the two recirculation zones by the 3D standard $k\text{-}\epsilon$ model on the different meshes used in this study is depicted in Figures 3 and 4 as streamlines and iso-surfaces plots respectively. To track the flow path at the recirculation flow regimes, streamlines are traced through different strategic locations depicted as small 3D pink colored spheres in Figure 3. These locations are going to be used to analyze streamlines throughout the current work.

From the figures, it can be observed that all types of meshes can capture the bluff-body induced RZ, whereas only H5 and H10 meshes are able to capture VB bubble as expected from the mesh analysis. However, it is to be noted that the predicted flow field on the H5 mesh is not symmetric about the geometric centerline of the flow passing through the center of the fuel jet. Hence, only the H10 mesh is capable of capturing both recirculation zones and symmetric feature of the flow field inside the burner. Furthermore, the scaled residuals of the solutions listed in Table 6 reveal that only the solution by H10 mesh meets the convergence criteria. Therefore, the H10 mesh can be nominated as the ideal candidate for further investigations.

Before continuing the investigation using the 10-zone hexahedron mesh (H10), a mesh independent study is carried out using 3.45, 1.5, 1.0, and 0.7 million cells. The line plot comparisons and streamlines of the velocity field along with axial velocity contours are shown in Figures 5 and 6 respectively. For all line plots, the axial position z is normalized by the bluff body diameter D = 50 mm and the radial position r is normalized by the radius of the jet hole R_j = 1.8 mm.

Analyzing the line plots, it can be observed there is no visible difference in the axial velocity predictions by different mesh resolutions. However, the contours of axial velocity and the streamlines shown in Figure 6 show deviations in upstream and downstream extent of the vortex breakdown (VB) bubble. Since a large number of cases are to be investigated for different 3D RANS models, the 1.0 million cells H103 mesh which gives a VB bubble of 15 mm is chosen over the 3.45 million cells H10 mesh which only gives a 2.5% bigger VB bubble despite having 71% more cells.

Velocity field comparison between measured LDV values and calculations using different schemes (as listed in Table 3) using the H103 mesh are shown in Figure 7. Interestingly, there is no significant difference in the line plots when second order upwind schemes are adopted. However, some minor differences can be observed at some locations when compared to the FFF scheme.

(a) T1 mesh   (b) T5 mesh   (c) H5 mesh

(d) T10 mesh   (e) H10 mesh
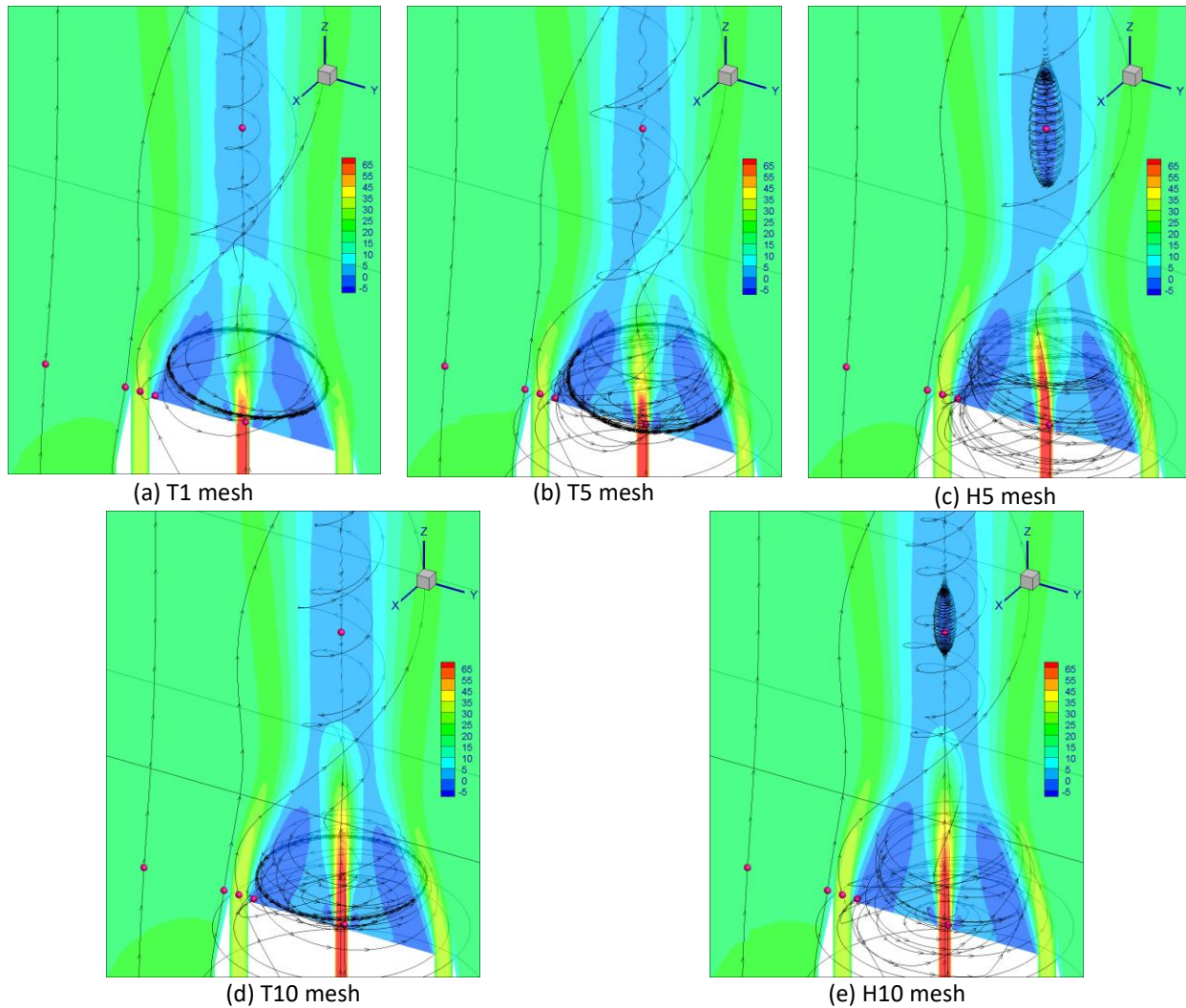
Fig. 3. Streamlines at selected locations (indicated by 3D pink-colored spheres) along with contour of axial velocity (m/s) at the centerline YZ-plane for different types of mesh

(a) T1 mesh   (b) T5 mesh   (c) H5 mesh

(d) T10 mesh   (e) H10 mesh
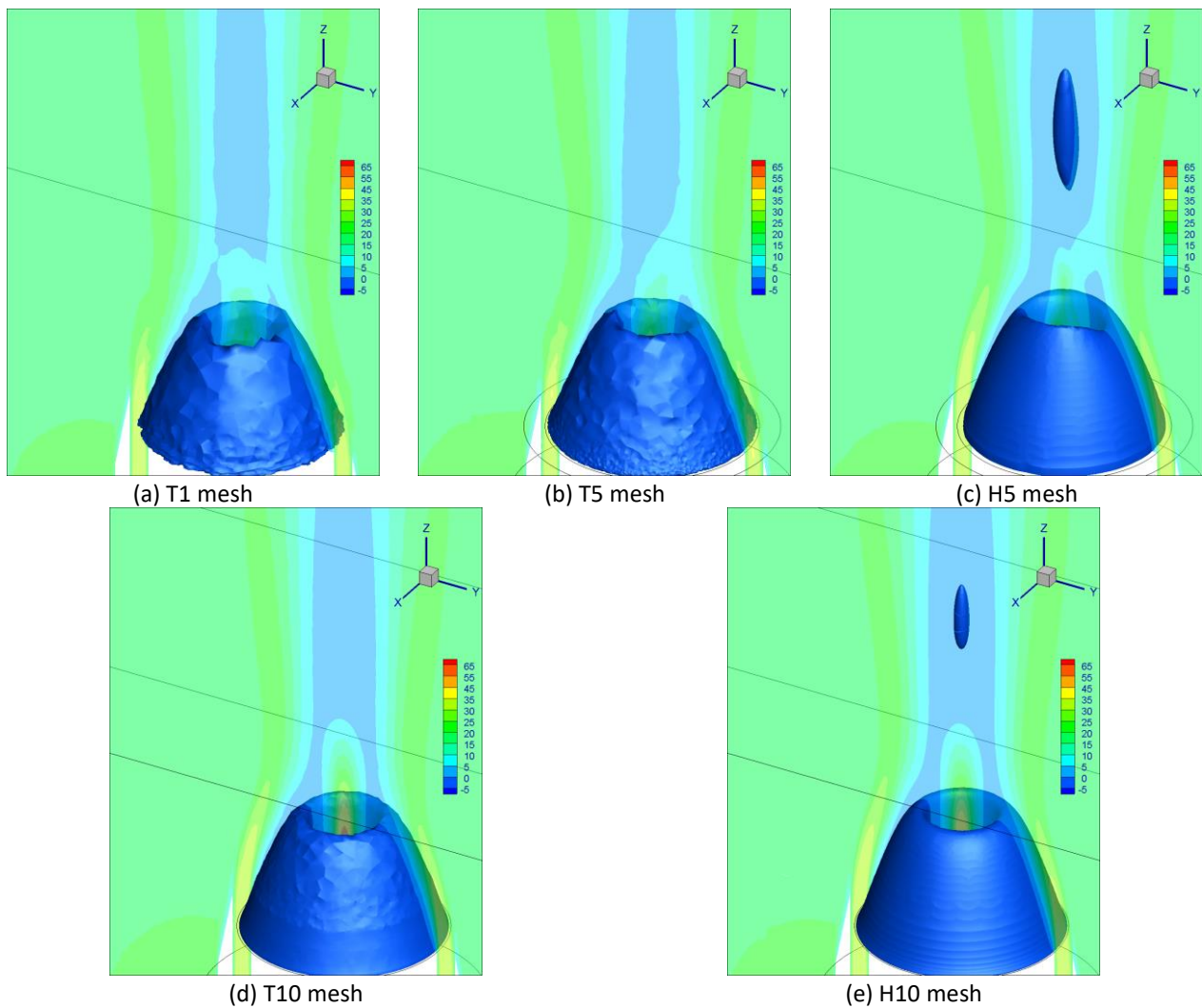
Fig. 4. Iso-surfaces of the recirculation zones (drawn at stagnation: 0 m/s) along with contour of axial velocity (m/s) at the centerline YZ-plane for different types of mesh

Table 6
Scaled residuals for various meshes after 7700 iterations

Scaled residuals	T1 mesh	T5 mesh	H5 mesh	T10 mesh	H10 mesh
Continuity	6.8098E-05	3.7297E-05	1.1336E-03	1.3923E-05	7.2928E-08
X-velocity	2.2479E-07	2.8103E-07	4.7170E-05	1.6006E-07	6.4386E-09
Y-velocity	2.1622E-07	3.0540E-07	5.0571E-05	1.7041E-07	7.5360E-09
Z-velocity	2.6526E-07	3.0508E-07	3.9374E-05	1.4710E-07	9.2194E-09
k	2.8334E-07	2.1256E-06	3.1474E-04	3.3682E-07	6.0524E-08
ϵ	1.4274E-06	6.3876E-06	2.5835E-03	1.0825E-06	3.4053E-07
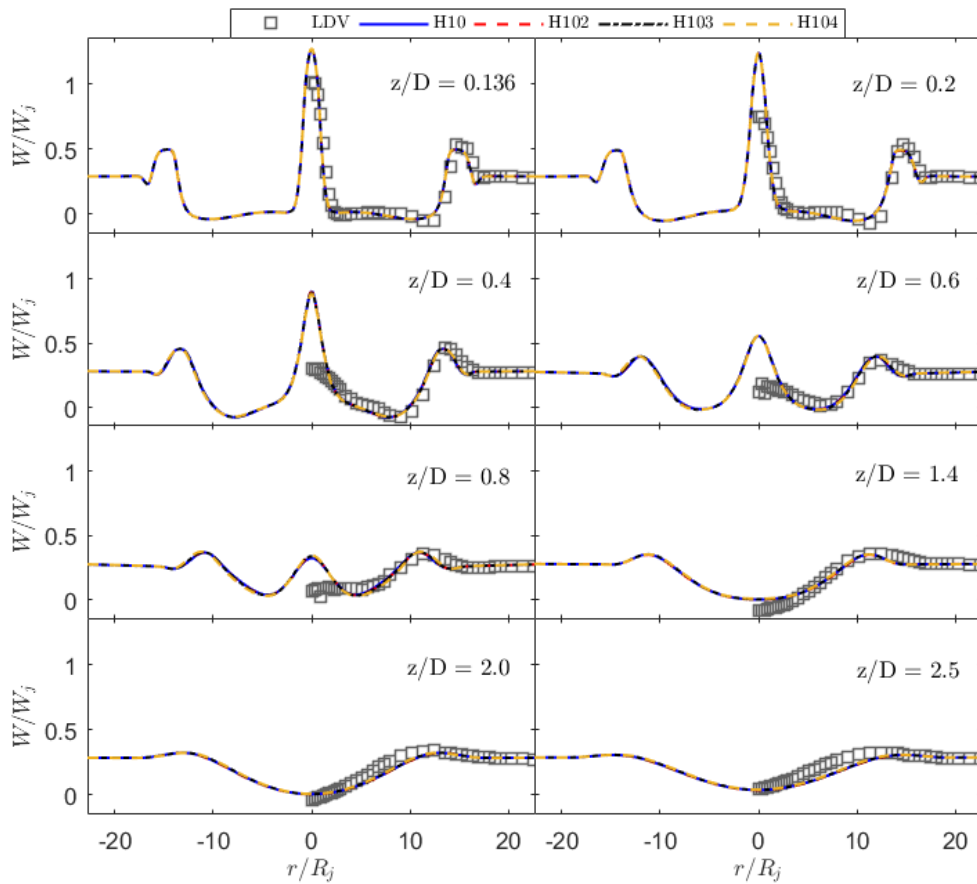
Fig. 5. Axial velocity versus radial direction at centerline YZ-plane with different distances from inlet. Comparison between experimental measurements (LDV) [2, 10] and computation using four different resolutions of the 10-zone hexahedron mesh: H10 (3.45M), H102 (1.5M), H103 (1.0M), H104 (0.7M)

(a) H10 mesh (3.45M)	(b) H102 mesh (1.5M)	(c) H103 mesh (1.0M)	(d) H104 mesh (0.7M)
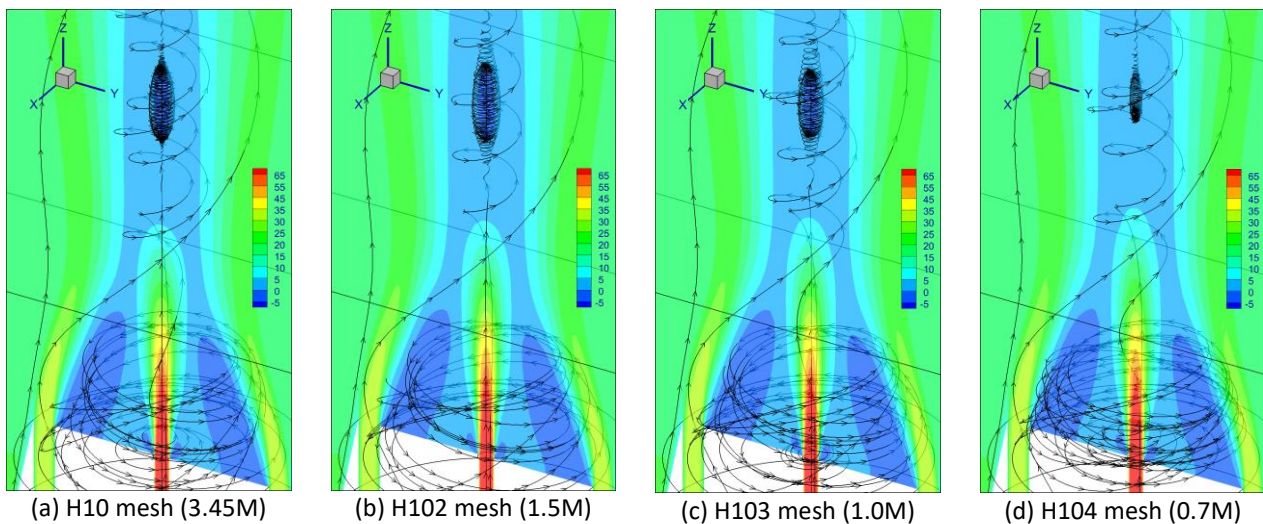
Fig. 6. Streamlines of recirculation zones along with contour of axial velocity (m/s) component at the centerline YZ-plane for different resolutions of the 10-zone hexahedron mesh

23
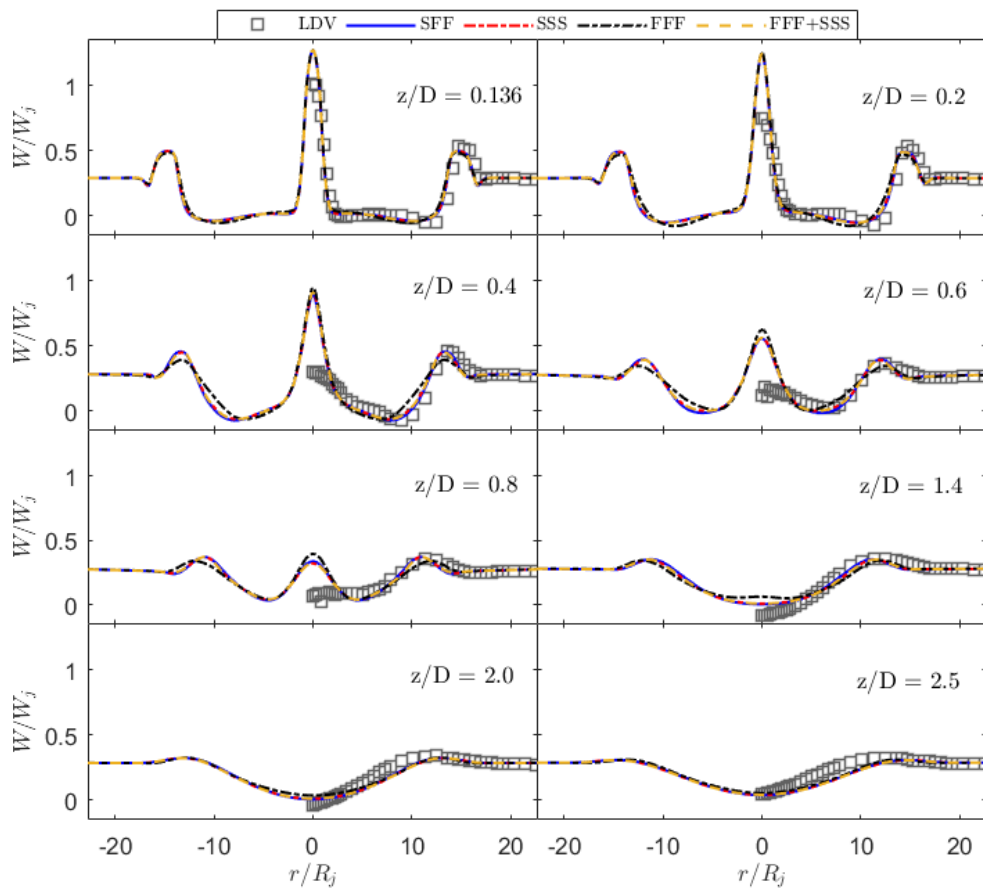
Fig. 7. Axial velocity versus radial direction at centerline YZ-plane with different distances from inlet. Comparison between experimental measurements (LDV) [2, 10] and computation by different discretization schemes using the H103 mesh

Although the line plots are not significantly different, nonetheless, the SFF (default) scheme is the only combination which can predict the VB bubble as depicted in Figure 8. Bluff-body induced recirculation zone and symmetric feature of the flow field are predicted by all schemes.

(a) SFF scheme (default)   (b) SSS scheme   (c) FFF scheme   (d) (FFF + SSS) scheme
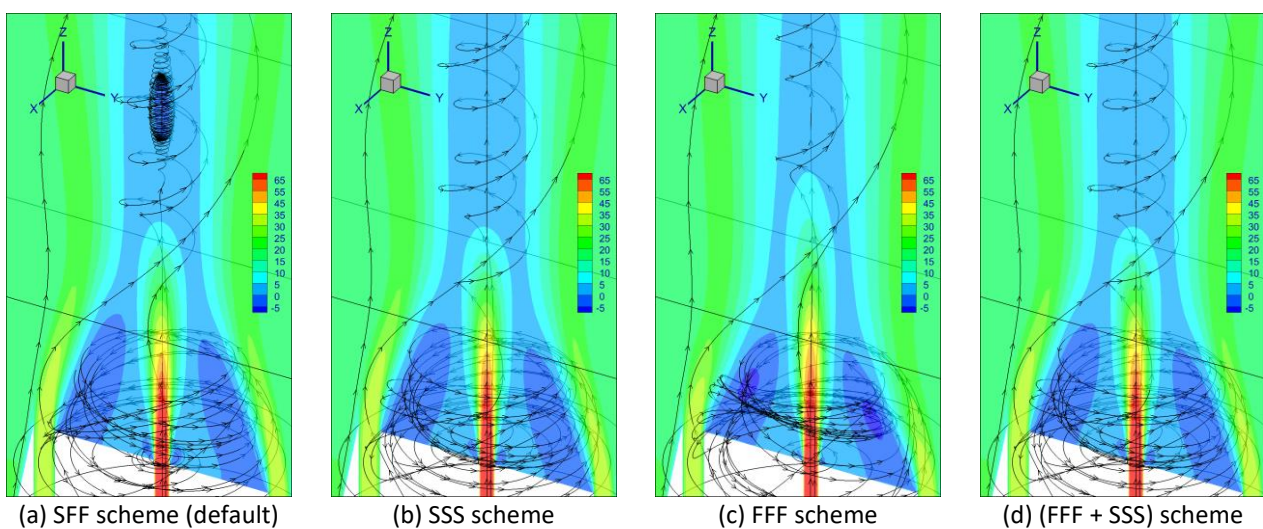
Fig. 8. Streamlines of recirculation zones along with contour of axial velocity (m/s) component at the centerline YZ-plane for different discretization schemes using the H103 mesh

Apart from investigating the effect of different spatial discretization schemes, five additional 3D RANS models, namely: realizable and RNG k-ϵ, standard k-ω, Transition-SST, and Reynolds stress model (RSM) are examined to study the influence of turbulence models on flow field predictions. Investigations using the standard k-ϵ model have provided important information on their feasibility in predicting the 3D swirl-stabilized isothermal turbulent flow field inside an industrial burner. It was found out that the ANSYS-Fluent default schemes provided better result. Therefore, the above mentioned five models are implemented to the current study by applying ANSYS-Fluent default scheme using the H103 mesh.

The streamlines and axial velocity contours predicted by all models are shown in Figure 9. It can be observed that only the 3D standard k-ϵ model is able to predict all the flow features of the swirl-stabilized turbulent flow.

(a) Standard k-ϵ model   (b) Realizable k-ϵ model   (c) RNG k-ϵ model

(a) Standard k-ω model   (b) Transition-SST model   (c) Reynolds stress model
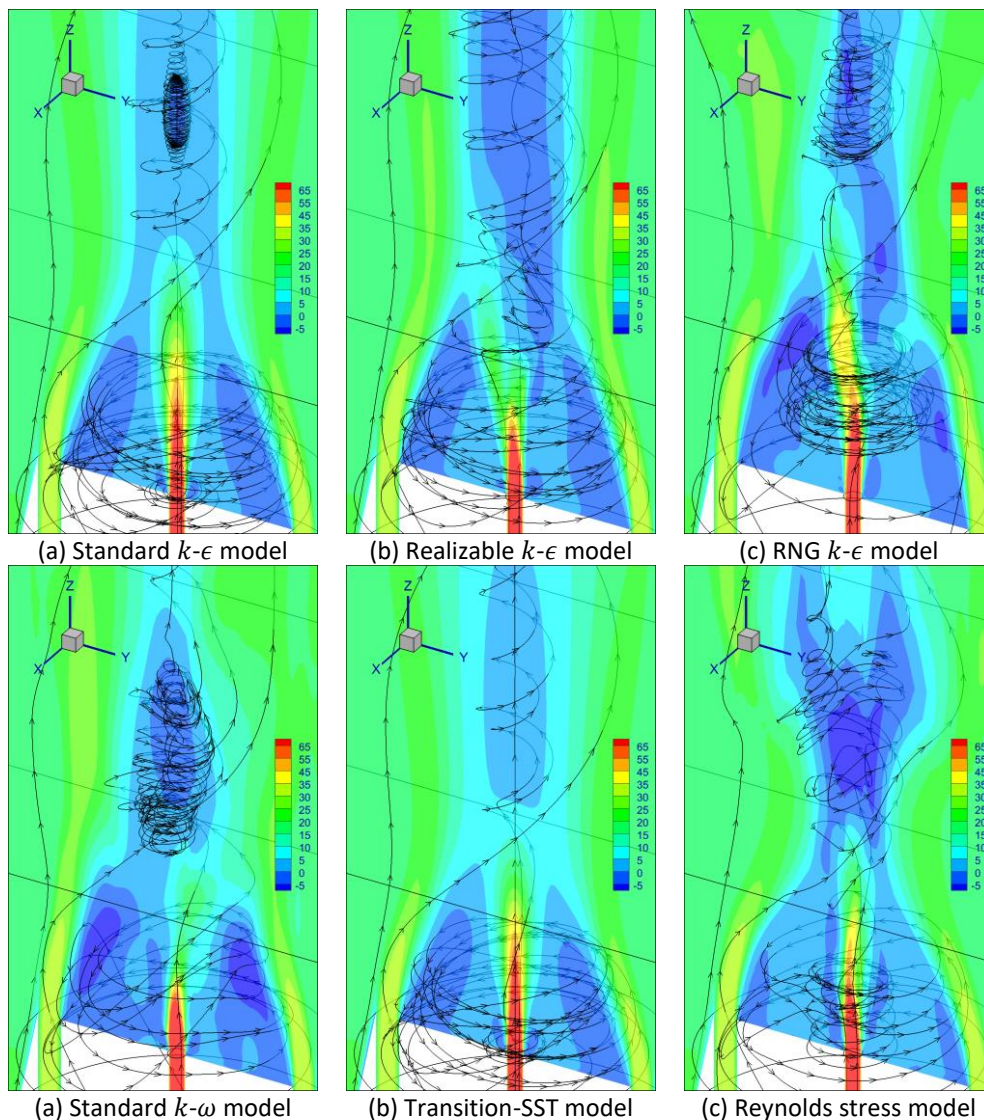
Fig. 9. Streamlines of recirculation zones along with contour of axial velocity (m/s) component at the centerline YZ-plane for different turbulence models using the H103 mesh

The other models except RSM, can predict the bluff-body induced recirculation zone but with asymmetric flow feature. The similitude of a VB bubble is visible in the predictions by RNG k-ϵ, standard k-ω, and Reynolds stress model (RSM) models whereas in the case of the realizable k-ϵ

model an axially stretched structure with recirculation feature can be identified. It is important to note that none of the solutions meet the convergence criteria except for the 3D standard k-ϵ model. Interestingly, the Transition-SST model is able to predict the symmetric flow feature along with the bluff-body induced recirculation zone although a weak VB bubble is predicted which could be related to mesh refinement, which makes it a candidate for further investigation.

It can be observed that (as shown in Figure 10) unlike the standard k-ϵ model, calculations of Transition-SST model using both H10 and H103 mesh fail to capture a distinct VB bubble although the bluff-body recirculation zone and symmetric feature of the flow field are predicted. It is also important to note that the residuals for these two calculations did not meet the convergence criteria. The influence of different discretization schemes listed in Table 7 on the Transition-SST model results was also tested and is shown in Figure 11. Like the case of standard k-ϵ model, a combination of FFFFF and SSSSS schemes was also investigated for the Transition-SST model.

(a) k-ϵ with H103 mesh   (b) T-SST with H103 mesh   (c) T-SST with H10 mesh
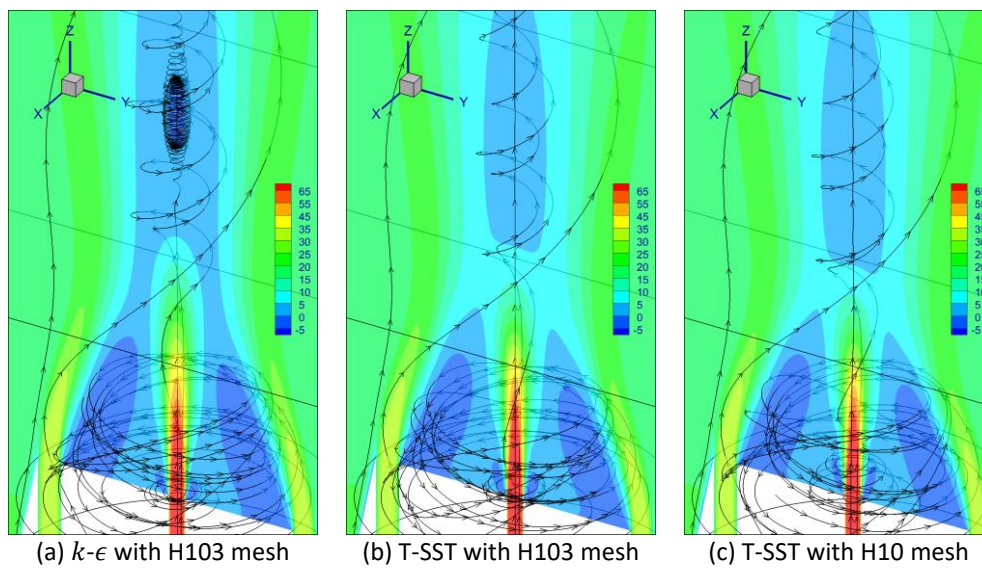
Fig. 10. Streamlines of recirculation zones along with contour of axial velocity (m/s) component at the centerline YZ-plane for different mesh resolutions of multi-zone (10-zone) hexahedron mesh using the standard k-ϵ model and Transition-SST model

Table 7
Upwind schemes for spatial discretization for the Transition-SST model

Scheme code	Momentum	Turbulent kinetic energy (k)	Specific dissipation rate (ϵ)	Intermittency	Momentum thickness Reynolds number
SFFFF (default)	Second order	First order	First order	First order	First order
SSSSS	Second order	Second order	Second order	Second order	Second order
FFFFF	First order	First order	First order	First order	First order

| (a) SFFFF scheme (default) | (b) SSSSS scheme | (c) FFFFF scheme | (d) (FFFFF + SSSSS) scheme |
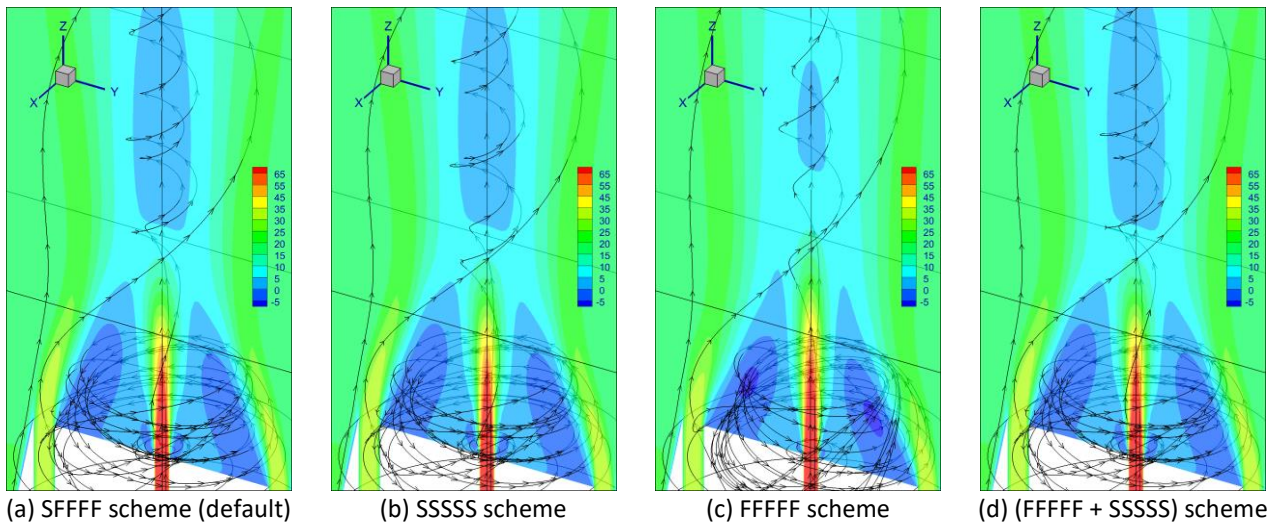
Fig. 11. Streamlines of recirculation zones along with contour of axial velocity (m/s) component at the centerline YZ-plane for different discretization schemes for the Transition-SST model using the H103 mesh

Analyzing Table 7 and Figure 11, it can be observed that similar to the case of standard k-ε model, adopting discretization schemes other than the default one for Transition-SST model do not bring any interesting change and improvement in the result.

5. Conclusions

In this work, a 3D swirl-stabilized isothermal turbulent jet was simulated using different 3D RANS models. In order to carry out the investigations, several types of meshes were generated. A brief mesh quality analysis based on several mesh metrics was also carried out to ensure the trustworthiness of the calculations using the meshes. Then by analyzing the results, the best mesh was chosen to carry out further investigations. The results of the current work are summarized in Table 8.

Analyzing Table 8, it can be concluded that the hexahedron mesh offers better prediction of the flow field as compared to the tetrahedron mesh. Mesh-independence study indicated that the hexahedron mesh can predict the flow field with significant accuracy despite having cell numbers as low as 0.7 million (H104). It was also found that adopting second order schemes to discretize all equations (for example SSS scheme for the standard k-ϵ model) do not necessarily result in better predictions, rather a combination of both the first and second order (for example SFF scheme for the standard k-ϵ model) schemes can provide better results.

It was found that the prominent flow features are predicted by at least two of the 3D RANS models, namely the standard k-ϵ and the Transition-SST. The standard k-ϵ model is able to predict a more prominent VB bubble as compared to all other turbulence models, although the extent of the VB bubble is not predicted correctly as can be seen from Table 9.

Table 8
Summary of simulations

Criteria	Mesh	Cell amount	Discretization Scheme	Solution Converged	Symmetric flow field	Bluff-body RZ	VB bubble
Standard k-ϵ model:							
	T1	1.67M	Default	✗	✗	✓	✗
	T5	1.73M	Default	✗	✗	✓	✗
	H5	2.29M	Default	✗	✗	✓	✓
Mesh type	T10	3.42M	Default	✗	✓	✓	✗
	H10	3.45M	Default	✓	✓	✓	✓
	H10	3.45M	Default	✓	✓	✓	✓
Mesh-independence study	H102	1.5M	Default	✓	✓	✓	✓
	H103	1.0M	Default	✓	✓	✓	✓
	H104	0.7M	Default	✓	✓	✓	✓
			SFF	✓	✓	✓	✓
Discretization Scheme			SSS	✓	✓	✓	✗
(default: SFF)	H103	1.0M	FFF	✓	✓	✓	✗
			FFF + SSS	✓	✓	✓	✗
Transition-SST model:							
	H10	3.45M	Default	✗	✓	✓	✗
Mesh-independence study	H103	1.0M	Default	✗	✓	✓	✗
			SFFFF	✗	✓	✓	✗
Discretization Scheme			SSSSS	✗	✓	✓	✗
(default: SFFFF)	H103	1.0M	FFFFF	✗	✓	✓	✗
			FFFFF + SSSSS	✗	✓	✓	✗
All models:							
Standard k-ϵ			Default	✓	✓	✓	✓
Realizable k-ϵ			Default	✗	✗	✓	✗
RNG k-ϵ			Default	✗	✗	✓	✗
Standard k-ω	H103	1.0M	Default	✗	✗	✓	✗
Transition-SST			Default	✗	✓	✓	✗
RSM			Default	✗	✗	✓	✗

Upstream and downstream extent of the VB bubble reported in other studies show that none of the 2D RANS simulations [8, 16, 18] can predict the VB bubble. Interestingly, one of the LES calculations [31] too could not predict the VB bubble supposedly for not having enough mesh resolution. Some LES calculations [4, 34, 17] predict the extent of the VB bubble quiet closely, while some overpredict [33] as much as 16 mm. For the current work, the standard k-ϵ model predicted an 18 mm VB bubble using the H102 mesh which was only 30% of the 60 mm size recorded in experimental data [2, 10]. The VB bubble obtained by the H103 mesh has a size of 15 mm which was only 1.7% less than the VB bubble predicted by the H102 mesh which had 50% more cells. Therefore, the standard k-ϵ model's predictions of the swirl-stabilized isothermal turbulent flow field with the moderate resolution mesh H103 (1.0 million cells) and using the default schemes (SFF) can be considered as a promising alternative to more computationally intensive methods like the LES, SAS, DES and to the less accurate 2D RANS methods. The inaccuracy involved in the prediction of the VB bubble extent can be attributed to the fact that an inherently unsteady flow is being predicted by a steady method. Hence it is likely that an unsteady RANS (URANS) approach with the standard k-ϵ model may increase the accuracy of predicting the VB bubble while being less computationally expensive than the traditional employed unsteady simulations like LES.

The conclusions in the paper are valuable, practical and will save a lot of time and effort of practicing engineers during the numerical modelling setup selection stages for solving such complex three-dimensional flow problems.

Table 9
Upstream and downstream extent of the VB bubble reported in different studies along with findings in current work

Works	Model	Cell amount in mesh	Approximate VB bubble start and end location (downstream to burner exit)	Upstream and downstream extent of the VB bubble
Al-Abdeli and Masri [2]	Experiment (LDV)	-	50 mm & 110 mm	60 mm
Malalasekera *et al.,* [4]	LES	1.0M	48 mm & 110+ mm	~ 62 mm
Kempf *et al.,* [29]	LES	1.0M	Captured	Not mentioned
Kempf *et al.,* [29]	LES	3.0+ M	Captured	Not mentioned
Stein and Kempf [30]	LES	1.82M	Captured	Not mentioned
Stein *et al.,* [31]	LES	0.46M	Not Captured	-
Olbricht *et al.,* [33]	LES	3.0M	35 mm & 111 mm	76 mm
Dinesh *et al.,* [34]	LES	3.0+ M	48 mm & 115 mm	67 mm
Yang and Kær [17]	LES	3.8+ M	48 mm & 102 mm	54 mm
Safavi and Amani [8]	LES, SAS, DES	2.7M	Captured	Not mentioned
De Meester *et al.,* [18]	2D k-ϵ	20.48K	Inaccurately captured [18]	Not mentioned
Radwan *et al.,* [16]	2D RANS	88.6K	Not captured	-
Safavi and Amani [8]	2D RANS	81K	Improperly captured [8]	Not mentioned
Findings in current 3D RANS investigation:				
T1 mesh		1.67M	Not captured	-
T5 mesh		1.73M	Not captured	-
H5 mesh		2.29M	64.5 mm & 97 mm	32.5 mm
T10 mesh	Standard k-ϵ	3.42M	Not captured	-
H10 mesh		3.45M	74.5 mm & 91 mm	16.5 mm
H102 mesh		1.5M	74 mm & 92 mm	18 mm
H103 mesh		1.0M	75 mm & 90 mm	15 mm
H104 mesh		0.7M	78 mm & 82 mm	4 mm
H10 mesh		3.45M	Not captured	-
H103 mesh	Transition-SST	1.0M	Not captured	-
	Realizable k-ϵ		Not captured	-
	RNG k-ϵ		Not captured	-
H103 mesh	Standard k-ω	1.0M	Not captured	-
	RSM		Not captured	-

References

[1] Kalt, Peter AM, Yasir M. Al-Abdell, Assaad R. Masri, and Robert S. Barlow. "Swirling turbulent non-premixed flames of methane: flow field and compositional structure." *Proceedings of the Combustion Institute* 29, no. 2 (2002): 1913-1919.

[2] Al-Abdeli, Yasir M., and Assaad R. Masri. "Recirculation and flowfield regimes of unconfined non-reacting swirling flows." *Experimental thermal and fluid science* 27, no. 5 (2003): 655-665.

[3] Al-Abdeli, Yasir M., Assaad R. Masri, Gabriel R. Marquez, and Sten H. Starner. "Time-varying behaviour of turbulent swirling nonpremixed flames." *Combustion and Flame* 146, no. 1-2 (2006): 200-214.

[4] Malalasekera, W., K. K. J. Ranga Dinesh, S. S. Ibrahim, and M. P. Kirkpatrick. "Large eddy simulation of isothermal turbulent swirling jets." *Combustion Science and Technology* 179, no. 8 (2007): 1481-1525.

[5] Dinesh, KKJ Ranga, K. W. Jenkins, A. M. Savill, and M. P. Kirkpatrick. "Swirl effects on external intermittency in turbulent jets." *International Journal of Heat and Fluid Flow* 33, no. 1 (2012): 193-206.

[6] Malalasekera, W., K. K. J. Ranga-Dinesh, Salah S. Ibrahim, and Assaad R. Masri. "LES of recirculation and vortex breakdown in swirling flames." *Combustion Science and Technology* 180, no. 5 (2008): 809-832.

[7] TNF Workshop Abstract, n.d. www.sandia.gov/TNF/abstract.html.

[8]   Safavi, Mohammad, and Ehsan Amani. "A comparative study of turbulence models for non-premixed swirl-stabilized flames." *Journal of Turbulence* 19, no. 10 (2018): 928–962.

[9]   Al-Abdeli, Yasir M., and Assaad R. Masri. "Precession and recirculation in turbulent swirling isothermal jets." *Combustion Science and Technology* 176, no. 5-6 (2004): 645-665.

[10]   Sydney swirl flow and flame database, n.d. web.aeromech.usyd.edu.au/thermofluids/swirl.php.

[11]   Masri, A. R., S. B. Pope, and B. B. Dally. "Probability density function computations of a strongly swirling nonpremixed flame stabilized on a new burner." *Proceedings of the Combustion Institute* 28, no. 1 (2000): 123-131.

[12]   Al-Abdeli, Yasir M., and Assaad R. Masri. "Stability characteristics and flowfields of turbulent non-premixed swirling flames." *Combustion Theory and Modelling* 7, no. 4 (2003): 731-766.

[13]   Masri, Assaad R., Peter AM Kalt, and Robert S. Barlow. "The compositional structure of swirl-stabilised turbulent nonpremixed flames." *Combustion and Flame* 137, no. 1-2 (2004): 1-37.

[14]   Al-Abdeli, Yasir M., and Assaad R. Masri. "Turbulent swirling natural gas flames: stability characteristics, unsteady behavior and vortex breakdown." *Combustion science and technology* 179, no. 1-2 (2007): 207-225.

[15]   Masri, A. R., P. A. M. Kalt, Y. M. Al-Abdeli, and R. S. Barlow. "Turbulence–chemistry interactions in non-premixed swirling flames." *Combustion Theory and Modelling* 11, no. 5 (2007): 653-673.

[16]   Radwan, Arabi, Kamal A. Ibrahim, Ahmed Hanafy, and Khalid M. Saqr. "On RANS modeling of unconfined swirl flow." *CFD Letters* 6, no. 4 (2014): 159-174.

[17]   Yang, Yang, and Søren Knudsen Kær. "Large-eddy simulations of the non-reactive flow in the Sydney swirl burner." *International Journal of Heat and Fluid Flow* 36 (2012): 47-57.

[18]   De Meester, Reni, Bertrand Naud, and Bart Merci. "Hybrid RANS/PDF calculations of Sydney swirling flames." In *4th European Combustion Meeting*. 2009.

[19]   Gupta, Amit, and Ranganathan Kumar. "Three-dimensional turbulent swirling flow in a cylinder: Experiments and computations." *International journal of Heat and fluid flow* 28, no. 2 (2007): 249-261.

[20]   West, Jonathan, Clinton P. Groth, and John Hu. "Assessment of Hybrid RANS/LES methods for gas-turbine combustor-relevant turbulent flows." In *22nd AIAA Computational Fluid Dynamics Conference*, p. 2921. 2015.

[21]   Widenhorn, Axel, Berthold Noll, and Manfred Aigner. "Numerical study of a non-reacting turbulent flow in a gas-turbine model combustor." In *47th AIAA Aerospace Sciences Meeting Including the New Horizons Forum and Aerospace Exposition*, p. 647. 2009.

[22]   Weber, R., B. M. Visser, and F. Boysan. "Assessment of turbulence modeling for engineering prediction of swirling vortices in the near burner zone." *International Journal of Heat and Fluid Flow* 11, no. 3 (1990): 225-235.

[23]   Wegner, B., A. Maltsev, C. Schneider, A. Sadiki, A. Dreizler, and J. Janicka. "Assessment of unsteady RANS in predicting swirl flow instability based on LES and experiments." *International Journal of Heat and Fluid Flow* 25, no. 3 (2004): 528-536.

[24]   Schneider, Christoph, Stefan Repp, Amsini Sadiki, Andreas Dreizler, and Johannes Janicka. "The effect of swirling number variation on turbulent transport and mixing processes in swirling recirculating flows: experimental and numerical investigations." In *TSFP DIGITAL LIBRARY ONLINE*. Begel House Inc., 2001.

[25]   Wu, Yajing, Christian Carlsson, R. Szasz, L. Peng, Laszlo Fuchs, and Xue-Song Bai. "Effect of geometrical contraction on vortex breakdown of swirling turbulent flow in a model combustor." *Fuel* 170 (2016): 210-225.

[26]   Dinesh, KKJ Ranga, M. P. Kirkpatrick, and Karl W. Jenkins. "Investigation of the influence of swirl on a confined coannular swirl jet." *Computers & Fluids* 39, no. 5 (2010): 756-767.

[27]   Bulat, G., W. P. Jones, and S. Navarro-Martinez. "Large eddy simulations of isothermal confined swirling flow in an industrial gas-turbine." *International Journal of Heat and Fluid Flow* 51 (2015): 50-64.

[28]   Stopper, Ulrich, Wolfgang Meier, Rajesh Sadanandan, Michael Stöhr, Manfred Aigner, and Ghenadie Bulat. "Experimental study of industrial gas turbine flames including quantification of pressure influence on flow field, fuel/air premixing and flame shape." *Combustion and Flame* 160, no. 10 (2013): 2103-2118.

[29]   Kempf, A., W. Malalasekera, K. K. J. Ranga-Dinesh, and O. Stein. "Large eddy simulations of swirling non-premixed flames with flamelet models: a comparison of numerical methods." *Flow, turbulence and combustion* 81, no. 4 (2008): 523-561.

[30]   Stein, Oliver, and Andreas Kempf. "LES of the Sydney swirl flame series: A study of vortex breakdown in isothermal and reacting flows." *Proceedings of the Combustion Institute* 31, no. 2 (2007): 1755-1763.

[31]   Stein, Oliver, Andreas M. Kempf, and Johannes Janicka. "LES of the Sydney swirl flame series: An initial investigation of the fluid dynamics." *Combustion science and technology* 179, no. 1-2 (2007): 173-189.

[32]   Dinesh, KKJ Ranga, and M. P. Kirkpatrick. "Study of jet precession, recirculation and vortex breakdown in turbulent swirling jets using LES." *Computers & Fluids* 38, no. 6 (2009): 1232-1242.

[33]   Olbricht, Clemens, Anja Ketelheun, Frederik Hahn, and Johannes Janicka. "Assessing the predictive capabilities of Combustion LES as applied to the Sydney flame series." *Flow, turbulence and combustion* 85, no. 3-4 (2010): 513-547.

[34] Dinesh, KKJ Ranga, Karl W. Jenkins, A. M. Savill, and M. P. Kirkpatrick. "Influence of bluff-body and swirl on mixing and intermittency of jets." *Engineering Applications of Computational Fluid Mechanics* 4, no. 3 (2010): 374-386.

[35] Hu, L. Y., L. X. Zhou, and Y. H. Luo. "Large-eddy simulation of the Sydney swirling nonpremixed flame and validation of several subgrid-scale models." *Numerical Heat Transfer, Part B: Fundamentals* 53, no. 1 (2008): 39-58.

[36] El-Asrag, H., and S. Menon. "Large eddy simulation of bluff-body stabilized swirling non-premixed flames." *Proceedings of the Combustion Institute* 31, no. 2 (2007): 1747-1754.

[37] James, S., J. Zhu, and M. S. Anand. "Large eddy simulations of turbulent flames using the filtered density function model." *Proceedings of the Combustion Institute* 31, no. 2 (2007): 1737-1745.

[38] Dinesh, KKJ Ranga, K. W. Jenkins, M. P. Kirkpatrick, and W. Malalasekera. "Modelling of instabilities in turbulent swirling flames." *Fuel* 89, no. 1 (2010): 10-18.

[39] Yang, Zhao, Xiangsheng Li, Zhenping Feng, and Li Chen. "Influence of mixing model constant on local extinction effects and temperature prediction in LES for non-premixed swirling diffusion flames." *Applied Thermal Engineering* 103 (2016): 243-251.

[40] Zhiyin, Yang. "Large-eddy simulation: Past, present and the future." *Chinese journal of Aeronautics* 28, no. 1 (2015): 11-24.

[41] Launder, Brian Edward, and Dudley Brian Spalding. "The numerical computation of turbulent flows." In *Numerical prediction of flow, heat transfer, turbulence and combustion*, pp. 96-116. Pergamon, 1983.